Radiative Corrections to Proton-Proton Fusion in Pionless Effective Field Theory

Evan Combes

Presented for CIPANP 2025

June 12, 2025

THE UNIVERSITY OF TENNESSEE
KNOXVILLE

A Long History of Study

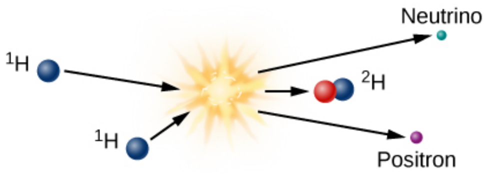

- Bethe's seminal work provided a qualitative understanding of proton-proton fusion. [Bethe, Phys Rev. 55, 1939]
- Proton-proton fusion continues to be studied in a number of frameworks, including chiral EFT and pionless EFT.

Why Radiative Corrections to Proton-Proton Fusion?

- Proton-proton fusion cross sections are important inputs for astrophysical models.
- Difficulty in experimentally measuring cross sections due to dominant Coulomb repulsion at low energies.
- Standing interest in quantifying uncertainties from radiative corrections. [Acharya et. al., Review Mod. Phys., 2025]

Recent Proton-Proton Fusion Calculations

- $S(0) = (4.100 \pm 0.024 \pm 0.013 \pm 0.008) \times 10^{-23}$ MeV fm^2. [Acharya et. al., J. Phys. G, 2023]
- $S(0) = (4.14 \pm 0.01 \pm 0.005 \pm 0.006) \times 10^{-23}$ MeV fm^2. [De-Leon and Gazit, Phys. Lett. B, 2023]
- Current quantifications of uncertainty due to radiative corrections places them around $\sim 1\%$. [Acharya et. al., Review Mod. Phys., 2025]
- Sirlin studied $\mathcal{O}(\alpha)$ corrections to single-nucleon beta decay and found it could be described by a single universal function. [Sirlin, Phys. Rev., 1967]
- We endeavor to perform explicit calculations of $\mathcal{O}(\alpha)$ corrections to proton-fusion and to explicitly quantify the leading contributions from nuclear structure.

Features of Pionless EFT

- S-wave Pionless EFT calculations have been performed in which the protons interact electromagnetically only with each other. [Kong and Ravndal, Phys. Rev. C, 2001]
- Pionless effective field theory utilizes a separation of scales to integrate pions out of the theory. Cutoff momentum of m_π.
- Pions in the physical theory are absorbed into contact and higher order derivative terms in $\not\pi$EFT.
- Pionless EFT is constructed to accomodate the unnaturally large proton-proton scattering length. [Kaplan, Savage, and Wise, Phys. Lett. B, 1998]
- Unambiguous power counting scheme.
- $$\mathcal{L}_{\not\pi} = N^\dagger \left(i\partial_0 + \frac{\nabla^2}{2m_N} \right) N - C_{0,s}(N^T \hat{P}_s N)^\dagger (N^T \hat{P}_s N) - C_{0,t}(N^T \hat{P}_t N)^\dagger (N^T \hat{P}_t N) + \ldots$$

Coulomb Interactions Between Protons

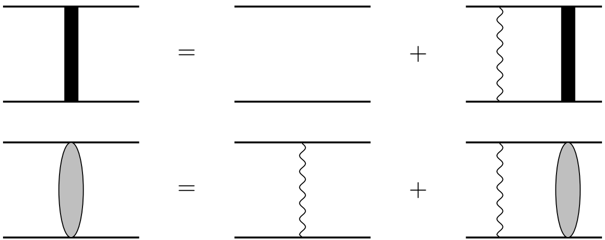

- Coulomb interactions between initial state protons:
  $\psi^+_{\mathbf{p}}(\mathbf{k}) = (2\pi)^3\delta^{(3)}(\mathbf{p}-\mathbf{k}) + \frac{t_C(E;\mathbf{k},\mathbf{p})}{E-\frac{\mathbf{k}^2}{2m_N}+i\varepsilon}$.
- Coulomb interactions between intermediate state protons:
  $G_C(E;\mathbf{k}_1,\mathbf{k}_2) = \frac{m_N}{(2\pi)^3}\int d^3\ell \frac{\psi^*_\ell(\mathbf{k}_1)\psi_\ell(\mathbf{k}_2)}{m_N E-\ell^2+i\varepsilon}$.
- The Coulomb wavefunction and Green's function handle electromagnetic interactions between protons to all orders.

E&M and Weak Lagrangians

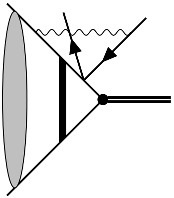

- $\mathcal{L}_{EM} = eN^\dagger \frac{1}{2}(1+\tau_3)NA_0 + e\bar{\Psi}_e\gamma^\mu\Psi_e A_\mu$.
- $\mathcal{L}_{weak} = -\sqrt{2}G_F V_{ud} g_V \bar{\Psi}_\nu \gamma^\mu \frac{1-\gamma_5}{2}\Psi_e (J^-_\mu)^{1b}$,
- $(J^-_\mu)^{1b} = V^-_\mu - A^-_\mu$.

Leading Order Diagrams and Amplitudes

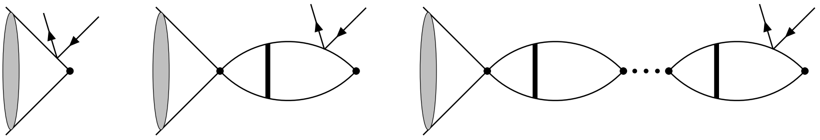

- Electromagnetic corrections to strong interactions. [Kong and Ravndal, Phys. Rev. C, 2001]

$$A(p) = \sqrt{8\pi\gamma_t} \int \frac{d^3k}{(2\pi)^3} \frac{\psi_{\mathbf{p}}^{+}(\mathbf{k})}{\gamma_t^2 + k^2} \ . \tag{1}$$

$$B(p) = \sqrt{8\pi\gamma_t} \int \frac{d^3k_1}{(2\pi)^3} \frac{d^3k_2}{(2\pi)^3} \frac{G_C(E; \mathbf{k}_1, \mathbf{k}_2)}{\gamma_t^2 + k^2} \ . \tag{2}$$

$$T_{fi}(p) = g_A \left[A(p) + \frac{C_{0,s}}{1 - C_{0,s}} \psi_{\mathbf{p}}^{+}(0) B(p) \right] \ . \tag{3}$$

THE UNIVERSITY OF TENNESSEE KNOXVILLE

Radiative Corrections Diagrams

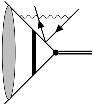

(d)

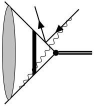

(e)

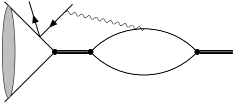

(f)

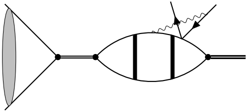

(g)

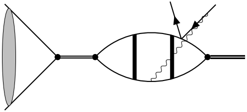

(h)

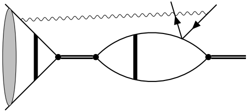

(i)

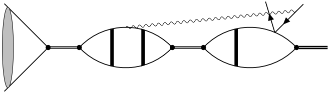

(j)

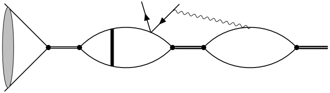

(k)

PP-Fusion Cross Section

$$\sigma(E) = \int \frac{d^3 p_e}{(2\pi)^3 2E_e} \frac{d^3 p_\nu}{(2\pi)^3 2E_\nu} 2\pi\delta(E + \Delta m - E_e - E_\nu)$$
$$\times \frac{1}{v_{\mathrm{rel}}} G_F^2 V_{ud}^2 |\langle d|A_-|pp\rangle|^2$$
$$\times F(Z, E_e)(1 + \Delta_R^V)(1 + \delta_R')(1 + \delta_{\mathrm{NS}}) \quad (4)$$

- $\langle d|A_-|pp\rangle$ pp-fusion amplitude with Coulomb interactions between only protons. [Kong and Ravndal, Phys. Rev. C, 2001]
- $F(Z, E_e)$ Fermi function, accounting for distortion of positron field due to final state deuteron.
- Δ_R^V corrections to single nucleon vector coupling, $1 + \Delta_R^V = 1.02471(25)$. [Cirigliano et. al., Phys. Rev. D, 2023]
- δ_R', δ_{NS} nuclear structure independent, dependent corrections.

Separation of Scales and Method of Regions

- Method of regions offers a prescription for handling loop integrals with strong separations of scales. [Beneke and Smirnov, Nuclear Physics B, 1998]
- Identify three photon momentum regions based on natural scales:
  - Ultrasoft; $q_0 \sim |\mathbf{q}| \sim E_e$,
  - Potential; $q_0 \ll |\mathbf{q}| \sim \gamma_t$.
- Loop energy integrals performed analytically. Only concerned about photon three-momentum scaling.
- In the ultrasoft region, we consider loop momenta to be much larger than photon momentum and so drop the photon momentum with respect to that.
- Potential photons estimated to contribute at $\mathcal{O}\left(\alpha \frac{E_e}{\gamma_t}\right)$, $\frac{E_e}{\gamma_t} \sim 0.01 - 0.02$. Numerical analysis supports this.

Example Application of Method of Regions

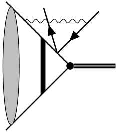

- $$i\mathcal{A}_1 = g_A\sqrt{8\pi\gamma_t}\int\frac{d^4q}{(2\pi)^4}\int\frac{d^3k_2}{(2\pi)^3}\int\frac{d^3k_1}{(2\pi)^3}L^j(q)$$
$$\times\frac{\psi^+_{\mathbf{p}}(\mathbf{k}_1)}{E'-\frac{\mathbf{k}_2^2}{m_N}+i\varepsilon}G_C\left(E+q^0-\frac{\mathbf{q}^2}{4m_N};\mathbf{k}_1-\frac{\mathbf{q}}{2},\mathbf{k}_2-\frac{\mathbf{q}}{2}\right)$$
- $L^j(q) = ie^2\bar{u}_\nu(p_\nu)\gamma^j P_L(\not{p}_e+\not{q}-m_e)\gamma^0 v_e(p_e)\frac{1}{\mathbf{q}^2}\frac{1}{(p_e+q)^2-m_e^2+i\varepsilon}$
- $$i\mathcal{A}\to g_A\sqrt{8\pi\gamma_t}\int\frac{d^4q}{(2\pi)^4}\int\frac{d^3k_2}{(2\pi)^3}\int\frac{d^3k_1}{(2\pi)^3}L^j(q)$$
$$\times\frac{\psi^+_{\mathbf{p}}(\mathbf{k}_1)}{E'-\frac{\mathbf{k}_2^2}{m_N}+i\varepsilon}G_C\left(E+q^0;\mathbf{k}_1,\mathbf{k}_2\right)$$

Ultrasoft Amplitude Result

$$\mathcal{A}_{\mathrm{us}} = g_A \left\{ \int \frac{d^4 q}{(2\pi)^4} \frac{L^j(q)}{q^0 + i\varepsilon} - i \int \frac{d^3 q}{(2\pi)^3} L^j(\mathbf{q}) \right\} T_{fi}(p) \qquad (5)$$

- First photon term is the virtual contribution to the Sirlin function. This is the function used in the one-body approximation. [Ando et. al., Phys. Lett. B, 2004]
- Second photon term, when taking the amplitude squared, is the $\mathcal{O}(\alpha)$ term in the Fermi function.
- When accounting for real emission, we determine δ'_R to arise from the Sirlin function.
- Validates prior use of the one-body approximation.
- $\delta'_R = 0.0163$.

Nuclear Structure Corrections

- Nuclear structure corrections are dominated by potential photons ($|\mathbf{q}| \sim \gamma_t$).
- Nuclear structure corrections arise from magnetic and weak-magnetic interactions.
  - $V_0^{(1)} = N^\dagger \frac{1+\tau^a}{2} N$,
  - $A_0^{(1)} = i g_A N^\dagger \tau_a \frac{\sigma \cdot (\overleftarrow{\nabla} - \overrightarrow{\nabla})}{m_N} N$,
  - $V_k^{(1)} = i N^\dagger \frac{1+\tau_a}{2} \frac{(\overleftarrow{\nabla}_k - \overrightarrow{\nabla}_k)}{2m_N} N - N^\dagger (\kappa^0 + \kappa^1 \tau_a) \epsilon_{kij} \frac{\sigma_i (\overleftarrow{\nabla}_j + \overrightarrow{\nabla}_j)}{2m_N} N$,
  - $A_k^{(1)} = g_A N^\dagger \frac{\tau^a}{2} \sigma_k N$,
  - $A_k^{(2)} = L_{1,A} (N^T \hat{P}_t^k N)^\dagger (N^T \hat{P}_s^a N) + \mathrm{h.c.}$.
- Consider only corrections up to $\mathcal{O}\left(\frac{1}{m_N}\right)$.

Leading Nuclear Structure Diagrams

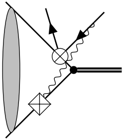

(l)

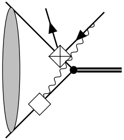

(m)

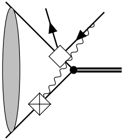

(n)

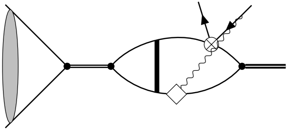

(o)

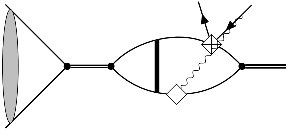

(p)

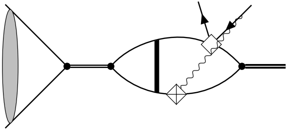

(q)

Leading Nuclear Structure Contributions

$$T^{(0)}_{\mathrm{mag}} = \sqrt{8\pi\gamma_t}\Bigg\{ \int \frac{d^3k_1}{(2\pi)^3} \int \frac{d^3k_2}{(2\pi)^3} \frac{1}{\mathbf{k}_1^2+\gamma_t^2} \psi^+_{\mathbf{p}}(\mathbf{k}_2) V^{(0)}_{\mathrm{mag}}(\mathbf{k}_1-\mathbf{k}_2)$$

$$+ \frac{4\pi}{m_N} D_{pp}(p)\psi^+_{\mathbf{p}}(0) \int \frac{d^3k_1}{(2\pi)^3} \int \frac{d^3k_3}{(2\pi)^3} \int \frac{d^3k_2}{(2\pi)^3} \frac{V^{(0)}_{\mathrm{mag}}(\mathbf{k}_1-\mathbf{k}_3)}{\mathbf{k}_1^2+\gamma_t^2} G_C(E;\mathbf{k}_2,\mathbf{k}_3) \Bigg\} \tag{6}$$

$$V^{(0)}_{\mathrm{mag}}(\mathbf{k}) = -\frac{4\pi}{m_N \mathbf{k}^2}\left(\frac{g_A}{3}(\kappa_0+\kappa_1) + \frac{1}{6}(\kappa_0-\kappa_1)\right) , \tag{7}$$

$$\delta_{\mathrm{NS}} = 2\alpha\left(T^{(0)}_{\mathrm{mag}} + T_{\mathrm{ct}}\right)\left[T^{\mathrm{LO}}_{fi}(p)\right]^{-1} . \tag{8}$$

Results and Summary

- Dominant ultrasoft photon contributions result in factorized hadron and photon components, yielding the product of the leading pp-fusion amplitude and Sirlin function.
- $(1+\Delta_R^V)(1+\delta_R') \rightarrow 1.04141(25)$.
- At most 0.2% correction to cross section from nuclear structure corrections.
- Additional calculations at yet higher orders are unlikely to offer corrections on even the percent level.
- Uncertainties in g_A and errors from truncation of the nuclear Hamiltonian are concluded to offer the greatest source of uncertainty in the cross section.